Development, Characterization and Sterilisation of Nanocellulose-Alginate-(Hyaluronic Acid)- Bioinks and 3D Bioprinted Scaffolds for Tissue Engineering

M. Lafuente-Merchan[1,2,3], S. Ruiz-Alonso[1,2,3], A. Espona-Noguera[1,2], P. Galvez-Martin[4,5], E. López-Ruiz[6,7,8], J.A. Marchal[6,7,9], M.L. López-Donaire[2,10], A. Zabala[11], J. Ciriza[1,2], L. Saenz-del-Burgo[1,2,3] * and JL. Pedraz[1,2,3*].

[1] NanoBioCel Group, Laboratory of Pharmaceutics, School of Pharmacy, University of the Basque Country (UPV/EHU), Vitoria-Gasteiz, Spain.

[2] Biomedical Research Networking Center in Bioengineering, Biomaterials and Nanomedicine (CIBER-BBN), Vitoria-Gasteiz, Spain.

[3] Bioaraba, NanoBioCel Research Group, 01009 Vitoria-Gasteiz, Spain

[4] R&D Human Health, Bioibérica S.A.U., Barcelona, Spain.

[5] Department of Pharmacy and Pharmaceutical Technology, Faculty of Pharmacy, University of Granada, Granada, Spain.

[6] Biopathology and Regenerative Medicine Institute (IBIMER), Centre for Biomedical Research, University of Granada, 18100 Granada, Spain.

[7] Instituto de Investigación Biosanitaria de Granada (ibs.GRANADA), Andalusian Health Service (SAS)—University of Granada, Granada, Spain.

[8] Department of Health Sciences, University of Jaén, 23071 Jaén, Spain.

[9] Department of Human Anatomy and Embryology, Faculty of Medicine, University of Granada, 18016 Granada, Spain.

[10] Institute of Polymer Science and Technology, ICTP-CSIC. Juan de la Cierva 3, 28006 Madrid, Spain.

[11] Surface Technologies, Mondragon University-Faculty of Engineering, Loramendi 4, 20500 Arrasate-Mondragon, Spain.

*Co-corresponding authors

Abstract

3D-bioprinting is an emerging technology of high potential in tissue engineering (TE), since it shows effective control over scaffold fabrication and cell distribution. Biopolymers such as alginate (Alg), nanofibrillated cellulose (NC) and hyaluronic acid (HA) offer excellent characteristics for use as bioinks due to their excellent biocompatibility and rheological properties. Cell incorporation into the bioink requires sterilisation assurance, and autoclave, β-radiation and γ-radiation are widely used sterilisation techniques in biomedicine; however, their use in 3D-bioprinting for bioinks sterilisation is still in their early stages. In this study, different sterilisation procedures were applied on NC-Alg and NC-Alg-HA bioinks and their effect on several parameters was evaluated. Results demonstrated that NC-Alg and NC-Alg-HA bioinks suffered relevant rheological and physicochemical modifications after sterilisation; yet, it can be concluded that the short cycle autoclave is the best option to sterilise both NC-Alg based cell-free bioinks, and that the incorporation of HA to the NC-Alg bioink improves its characteristics. Additionally, 3D scaffolds were bioprinted and specifically characterized as well as the D1 mesenchymal stromal cells (D1-MSCs) embedded for cell viability analysis. Notably, the addition of HA demonstrates better scaffold properties, together with higher biocompatibility and cell viability in comparison with the NC-Alg scaffolds. Thus, the use of MSCs containing NC-Alg based scaffolds may become a feasible tissue engineering approach for regenerative medicine.

Keywords: 3D-bioprinting, sterilisation, bioinks, tissue engineering.

1. Introduction

Three-dimensional (3D) bioprinting is an emerging additive manufacturing technology with great potential for use in the field of tissue engineering (TE) and regenerative medicine.[1] 3D-bioprinting is also applied in the development of drug screening models, as well as tumor models and cell-based sensors.[2] Among tissue fabrication techniques, 3D-bioprinting has the advantage of being precise in simulating native tissues and mechanical properties. As a result, a great deal of progress has been achieved in the fabrication of tissues such as bone in which mechanical characteristics are highly important.[3,4] Additionally, scaffolds to cartilage regeneration have been widely studied too. In fact, scaffolds to regenerate articular cartilage have been achieved *in vitro*.[2,5] One of the tissues in which this technology has focused most is the skin. It has been reported many available literature with *in vivo* results, which printed skin substitutes for wounds and burns has been successfully obtained.[3,6,7] On the other hand, it has been applied in more complex structures such as cornea,[8] heart[9] and tendon.[10] However, despite the emerging increase in their usage, there is little information about its step forward to clinical practice. Thus, more research is still needed.

This technology is based on the deposition of a biomaterial embedded with cells in a previously arranged form, in order to create complex structures that mimic native biological tissues.[1,2] This mixture of one or more biomaterials, together with the cells of interest depending on the application, is known as bioink, and requires specific rheological and mechanical properties, so it can be used as bioprinting material. In addition, bioinks must be non-toxic and biocompatible,[2,11] given that bioprinted scaffolds final purpose is their use in clinical practise.

These biological and medical applications require a compulsory sterilisation step so that the scaffolds do not cause infections in the clinics.[12] Furthermore, unlike other medical devices that are sterilised in a final step before their biological applications,[13] bioinks must be sterilised prior to the incorporation of the cellular component, which is usually carried out just before the bioprinting procedure itself. However, despite the importance of this sterilisation step, the alternatives for sterilising different biomaterials have been poorly studied.

Common sterilisation techniques have focused on achieving the highest degree of elimination of pathogens. Nevertheless, for 3D-bioprinting, not only must sterility be ensured, but also the procedure should not be too aggressive for the biomaterials that constitute the bioinks. Among the sterilisation techniques filtration, high temperatures, gases and radiation have been applied for the sterilisation of hydrogels used for regenerative medicine.[12] However, the high viscosity values that bioinks need to meet in order to be processed by the 3D printer, render filtration technique difficult to implement. On the other side, bioinks containing biomaterials sensitive to temperature can be damaged after being exposed to high temperatures by using autoclave.[11,14] As an alternative, the use of gases, such as ethylene oxide, have safety issues in terms of flammability, highly toxic residues and cancerous nature that must be taken into account.[12,15,16] In this context, Ultra-Violet light (UV), gamma (γ) radiation and beta (β) radiation have been applied for this purpose.[16-20] Ionising radiations have shown good assurance of sterility,[11,16] no chemical residues[15] and immediate results.[16] Yet, γ-radiation and β-radiation require complex application procedures and have an elevated cost,[16] whereas UV sterility assurance is dubious in value due to the low penetration capacity in highly viscous bioinks.[17]

After this review of the commonest methods of sterilisation, and given the little information available in the literature regarding the application of different sterilisation procedures to obtain safe bioinks, we planned to carry out an in-depth study of the effects of the application of the most promising sterilisation techniques, such as heat and radiation, onto bioinks composed of nanofibrillated cellulose (NC), sodium alginate (Alg) and hyaluronic acid (HA).

These biomaterials have been widely applied in biomedicine with promising results in different areas. NC is characterised by its high water content capacity, good biocompatibility and excellent physical and chemical properties.[18,19] Furthermore, it has stood out in different applications as drug and protein delivery,[20] gene therapy[21] and wound healing.[22] On the other hand, Alg has become one of the most studied biopolymers in 3D-bioprinting.[23,24] It offers fast gelling capacity when it is mixed with divalent cations, such as calcium, which enables the manufacturing of manageable scaffolds after bioprinting.[23] Furthermore, its high biocompatibility makes it the ideal material for 3D-bioprinting.[2,11,23,25] The NC and Alg mixture as a bioink has been applied for the fabrication of 3D bioprinted scaffolds for cartilage

regeneration as NC mimics the bulk collagen matrix of the cartilage tissue and Alg hydrogels have been reported to regenerate cartilage in vivo.[2,26,27]

Additionally, HA has been often used both to modify the bioinks rheological properties in order to favour the bioprinting process and in the fabrication of hydrogels for regenerative medicine. It has shown excellent biodegradability as well as biocompatibility properties,[18,28-30] and is involved in many biological processes such as cell adhesion,[18,29] migration and growth,[31,32] as well as in inflammatory processes and wound healing.[29,33,34] In addition, HA is a major component of native cartilage and it has been reported that controls chondrocyte metabolism and cartilage regeneration.[29] In fact, HA together with NC and Alg, has been applied for the fabrication of hydrogels and 3D printed structures for cartilage regeneration.[2,35] Furthermore, NC-Alg based hydrogels have resulted in gradual extracellular matrix formation and cartilage regeneration *in vivo* in nude mice models.[36]

Acknowledging the importance of selecting the best biomaterials to develop specific bioinks for 3D-bioprinting, as well as the relevance of choosing the correct sterilisation technique, this study is focused on evaluating the effect of three different sterilisation methods on these highly often employed materials. Two modalities of autoclaving (short and long cycle), as well as the sterilisation by β- and γ-radiation were used. Then, the effect of these procedures on the main properties of the biomaterials were analysed, as they are crucial for a correct printing. Next, an evaluation of whether the sterilised NC-Alg based bioinks (NC-Alg and NC-Alg-HA bioinks) in the manufacturing of 3D printed scaffolds that may be useful for regenerative medicine purposes was conducted. Finally, NC-Alg and NC-Alg-HA bioinks were loaded with murine D1 mesenchymal stem cells (D1-MSCs) before printing and the biological response of these cells included in 3D printed scaffolds was evaluated.

2. Materials and Methods

2.1. Materials

Ultra-pure low-viscosity high guluronic acid sodium alginate (UPLVG) (Mw>200 kDa) was purchased from FMC Biopolymer (Sandvika, Norway). Hyaluronic acid (Mw 600-

800 kDa) was obtained from Bioiberica (Barcelona, Spain). Nanofibrillated cellulose was purchased from Sappi Europe (Brussels, Belgium). D-mannitol, calcium chloride and 3-(4,5-dimethylthiazol-2-yl)-2,5-diphenyltetrazoliumbromid (MTT) *in vitro* toxicology assay were purchased from Sigma-Aldrich (Madrid, Spain). Fetal bovine serum (FBS), fetal calf serum (FCS) and penicillin/streptomycin (P/S) were purchased from Fisher Scientific (Madrid, Spain). DPBS code BE17-513F was purchased from Lonza (Porriño, Spain). Alamar blue was purchased from Bio-Rad científica (Madrid, Spain). LIVE/DEAD® Viability/Cytotoxicity kit was purchased from Life Technologies (Madrid, Spain).

2.2. Bioinks preparation

Two different bioinks were prepared. Nanocellulose-alginate (NC-Alg) and nanocellulose-alginate-hyaluronic acid (NC-Alg-HA) bioinks.

For the NC-Alg bioink, first, a 10 % (w/v) Alg solution was prepared in D-mannitol (1 %). Then, NC was added and mixed until complete homogenization. The final bioink proportion of NC:Alg was 80:20 (v/v), and the final concentration of Alg in the NC-Alg bioink was 2 % (w/v).

In order to prepare the NC-Alg-HA bioink, Alg and HA were dissolved in a D-mannitol solution to make an initial 10 % (w/v) and 5 % (w/v) solution, respectively. Then, NC was added and mixed until complete homogenization. The final bioink proportion of NC:Alg-HA was 80:20 (v/v), and in the NC-Alg-HA bioink the final concentration of Alg was 2 % (w/v) and the concentration of HA was 1 % (w/v). Afterwards, bioinks were stored at 4 ºC.

2.3. Sterilisation

Three sterilisation techniques were studied for each cell-free bioink: autoclave which includes short cycle and long cycle procedures, β-radiation and γ-radiation. For each technique 5-10 mL were sterilised by depositing the bioinks into closed sterile syringes.

2.3.1. Sterilisation by short cycle autoclaving

This process was performed by AJL Ophthalmic (Miñano, Spain) in an industrial autoclave F0A2/B model. This autoclaving process was carried out for 54 min. The

cycle started at 0.96 bar pressure and 15-18 °C temperature. Next, for 22 min the pressure and temperature increased until being set at 3.70-3.60 bar and 123-124 °C, respectively. The sterilisation occurred with these parameters set for 3.04 min. Afterwards, refrigeration process occurred and pressure and temperature decreased to 1.60 bar and 50-55 °C for 26 min. Finally, the cycle finished after 54 min with 1.05 bar pressure and around 50 °C temperature.

2.3.2. Sterilisation by long cycle autoclaving

The long cycle autoclaving process was performed in a clean autoclave ST DRY PV-II 75 L from Biotech (Barcelona, Spain). The sterilisation step occurred at 2 bar pressure and 121 °C for 30 min followed by an atmospheric purge in which pressure decreased around 0 bar and temperature was maintained at 121 °C. The whole process was carried out in 80 min. **Figure 1** shows the differences between short and long cycle autoclaving processes.
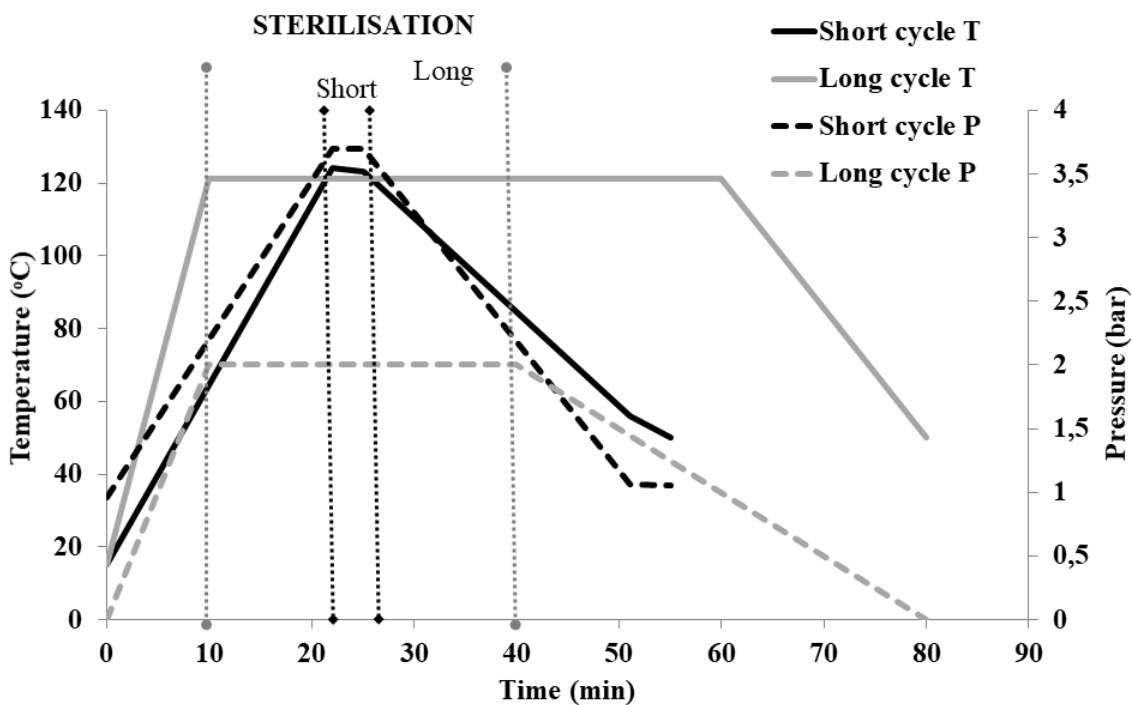

Figure 1. Comparison between short cycle and long cycle autoclaving procedures.

2.3.3. Sterilisation by β-radiation

β-radiation was performed according to ISO 11137 by Ionisos Iberica (Cuenca, Spain). [37] The samples were irradiated by a Rhodotron TT200, capable of generating a beam with energy of 10 MeV and a maximum power of 80 kW. The speed of the samples

going under the beam was adjusted to guarantee the minimum dose of 25 kGy and homogeneity of dose was ensured by passing the samples twice.

2.3.4. Sterilisation by γ-radiation

The sterilisation of the samples by γ-radiation was performed in a Mark I-30 137Cs irradiator from J.L. Shepherd and Associates (San Fernando, United States). The system was calibrated by relative film dosimetry using Gafchromic EBT3 film as a dosimetry system. The average dose rate was 3.2 Gy·min^{-1} for radiation position. A dose rate is used for calculating radiation exposure times until achieving the required total dose, 25 kGy.

2.4. Sterility Testing

Sterility testing was conducted for NC-Alg and NC-Alg-HA cell-free bioinks after being sterilised by short and long cycle autoclaving procedures, β-radiation and γ-radiation.

The test was carried out by direct inoculation of 1 mL of sample (bioink) in the microbiology medium to test for the growth of yeast, fungi, aerobic, and anaerobic bacteria according to the European Pharmacopoeia.[38] Two microbiological media were used: Thioglycollate Penase Broth (9 mL) (TPB) to detect anaerobic and aerobic bacteria, and Tryptic Soy Penase Broth (9 mL) (TSPB) which is a soybean casein digest medium, to detect fungi and aerobic bacteria, both were purchased from VWR International (Radnor, United States). For each media (TPB and TSPB), sterility test and growth promotion test of aerobes, anaerobes and fungi were previously verified. The inoculated media with each bioink were incubated for 14 days at 35 ºC and 22 ºC for TPB and TSPB respectively. All samples were visually inspected every day to observe if media showed turbidity. After 14 days, if there had been microbial growth, the medium would have shown turbidity. This assay was performed under aseptic conditions inside a safety cabinet in a clean room.

2.5. Bioinks characterization

2.5.1. Rheological study

Rheological properties were measured at room temperature using the rheometer AR1000 from TA Instruments (New Castle, United States) with a flat stainless steel plate of 40 mm geometry. Two different rheological measurements were performed: viscosity and viscoelasticity. In the steady flow measurement, viscosity was evaluated through a shear rate sweep from 0.1 to 100 s^{-1} followed by a second sweep from 100 to 0.1 s^{-1}. In addition, to study the bioinks viscoelasticity (storage modulus (G') and loss modulus (G'')), 2 % strain was set and the oscillation frequency sweeps were established from 0.1 to 100 Hz.

2.5.2. Macroscopic characteristics, osmolality and pH determination

The physical appearance of the bioinks was inspected visually before and after sterilisation. Macroscopic aspect and colour were evaluated.

Osmolality was determined by the cryoscopic osmometer Osmomat 030-D Gonotec (Berlin, Germany). In this assay, 50 µL of each bioink was analysed by determining the freezing depression point.

The pH was determined by pH-meter GLP 21 from Crison (Barcelona, Spain). Each sample was studied in triplicate.

2.6. 3D-printing

The bioinks were printed using an extrusion-based 3D bioprinter Bio X from Cellink (San Carlos, United States). Circular grid-like scaffolds of 14 mm diameter and 4 layers were printed through a 27 G conical nozzle. Printing parameters were set depending on the bioink. For NC-Alg bioink 4 mm/s printing speed and 20-22 kPa extrusion pressure was required. On the other hand, 4 mm/s printing speed and 24-26 kPa extrusion pressure were set for the NC-Alg-HA bioink. Finally, printed scaffolds were submerged in a 100 mM calcium solution in order to perform the crosslinking procedure.

2.7. Scaffolds characterization

2.7.1. Scanning electron microscopy (SEM)

Samples were coated with a thin layer of gold ($\sim$ 15 nm) using an Emitech K550X ion-sputter after critical point drying. Then, samples were observed in a S-3400 Scanning

Electron Microscope from Hitachi (Elk Grove Village, United States). The voltage used was 15 kV and the working distance was around 20 mm.

2.7.2. Surface and architectural structure study

The surface topography and architecture of the scaffolds were characterized using an optical profilometer from Sensofar S-NEOX (Barcelona, Spain) through focus variation method. The measurements were post-processed using the metrological software SensoMAP Premium 7.4 from Digital Surf (Besançon, France). The scaffolds were characterized in hydrated state after wiping with a dry lint free wipe.

For architectural study, a measurement of 6484x4880 μm^2 area at 3 locations on 3 independently printed samples for each condition were acquired using a 10x objective (lateral sampling: 1.29 µm, vertical resolution: 25 nm). The deposited strut height and thickness were characterized and the deposited material volume was computed through the 3D parameter Vm.[39] Finally, measurements were binarized, and the aspect ratio (Dmax/Dmin) was computed in order to characterize the grid morphology. Surface topography was characterized based on measurements of 873x656 μm^2 acquired at 3 different locations with a 20x objective (lateral sampling: 0.65 µm, vertical resolution: 8 nm). 3D topographical parameters belonging to height (Sq), spatial (Sal) and hybrid (Sdr) from ISO 25178-2[40] were computed on cropped areas of 150x150 μm^2.

2.7.3. Swelling

To evaluate the swelling behaviour, 0.6x14 mm^2 NC-Alg and NC-Alg-HA scaffolds were printed. Then, the scaffolds were lyophilized in Telstar cryodos Freeze Dryer (Terrassa, Spain) and weighted in order to obtain the dried weight. Dried scaffolds were immersed in Dulbecco's phosphate-buffered saline (DPBS) with calcium and magnesium at 37 °C to estimate their swelling capacity. At selected time points, scaffolds were removed from DPBS, water excess was removed using filter paper and then scaffolds were reweighed. The swelling in % was calculated in every time point by using the following equation:

$$\text{Swelling (\%)} \frac{W_{wet}-W_{dried}}{W_{dried}} \times 100$$

Where W_{wet} and W_{dried} correspond to wet and dried weight, respectively.

2.7.4. Degradation study

To evaluate the degradation process, the 3D printed NC-Alg and NC-Alg-HA scaffolds area were measured. Scaffolds were placed in DMEM at 37 °C and, at selected time points, they were measured again. After performing the measurements, scaffolds were returned to the culture medium. The area loss in % was calculated by using the following equation:

$$\text{Area loss (\%)} \frac{A_{before}-A_{after}}{A_{before}} \times 100$$

Where A_{before} and A_{after} correspond to the scaffold area before introducing it in DMEM and after passing selected time inside the media.

2.8 Biological studies of bioprinted scaffolds

2.8.1. Cytotoxicity assay

In vitro cytotoxicity test was determined according to ISO 10993-5-2009.[41] Adhesion, indirect and direct methods were performed to evaluate potential cytotoxicity of bioinks in mouse L929 fibroblasts. Disks were bioprinted following the aforementioned procedure (see section 2.6). Cells were cultured in complete media and seeded at a cell density of 3.123×10^4 cells/cm^2.

In the adhesion assay, NC-Alg and NC-Alg-HA bioprinted disks were set on 24 well plates and cells were seeded on top of them. Then, after 4 h of incubation, cell viability was measured using the MTT *in vitro* toxicity assay following manufacture's recommendations. Cells directly seeded onto the plate were used as controls.

In the indirect method assay, bioprinted disks were incubated with DMEM for 24 hours to obtain a conditioned media and cells were seeded at the same density as before onto independent wells. Then, disks were removed and the conditioned media was added to the cells. In direct method assay, cells were also seeded and cultivated for 24 hours onto culture plates and exposed directly to the printed disk by placing them onto seeded cells. After 24 hours of incubation, cell viability was measured in both assays using the same

MTT procedure. Cells not exposed to conditioned media or cells with no bioprinted disk exposure were used as controls.

In all assays, the absorbance was recorded using an Infinitive M200 microplate reader from TECAN Trading AG (Männedorf, Switzerland) at 570 nm with reference wavelength set at 650 nm.

Cell viability was calculated using the following equation:

$$\text{Cell viability (\%)} \frac{\text{Testing sample OD}_{570}}{\text{Untreated blank OD}_{570}} \times 100$$

Six independent experiments were conducted with three replicates per experiment. Cell viability above 70% was considered as non-toxic according to ISO 10993-5-2009.

2.8.2. D1-MSCs culture conditions and 3D-bioprinting

Murine D1-MSCs from ATCC (Virginia, United States) were cultured in T-flasks with DMEM supplemented with 10 % (v/v) FBS and 1 % (v/v) P/S. They were maintained at 37 °C in a humidified atmosphere containing 5 % CO_2. Medium was regularly changed. At 80 % of confluence, cells were subcultured.

For the 3D-bioprinting process, cells were incorporated and resuspended in the bioinks at 2.5×10^6 and 5×10^6 cell/mL density. Then they were bioprinted following the previously explained procedure (see section 2.6). Immediately after this, bioprinted scaffolds were crosslinked by adding a 100 mM $CaCl_2$ solution. These constructs were kept in the calcium solution for 5 min after which they were cultured in a complete medium. This whole process was performed at room temperature, under aseptic conditions.

2.8.3. Metabolic activity determination

The metabolic activity of the embedded D1-MSCs was determined weekly using the AlamarBlue® assay (AB). 14 mm circular grid-like bioprinted scaffolds were placed in 24 well plates with the solution containing 10 % of AB in complete medium and then, they were incubated for 24 hours at 37 °C. The fluorescence was read on an Infinite M200 microplate reader from TECAN Trading AG (Männedorf, Switzerland) at

excitation 560 nm and 590 nm emission wavelength. Wells containing culture media were used as negative controls. At least five wells were placed for each condition.

2.8.4. Cell viability qualitative determination by fluorescence microscopy

Cell viability determination was carried out weekly using the LIVE/DEAD® Viability/Cytotoxicity Kit. Constructs were washed four times with DPBS before performing the staining with 100 mM calcein AM in DPBS on 24 well plates for 40 min at room temperature in the dark. Then, the calcein solution was removed and a 0.8 µM ethidium homodimer-1 solution was added. The constructs were incubated for another 10 min at 37 °C and then, they were washed again with DPBS. Next, samples were observed under a Nikon TMS microscope (Hampton, United States) with the excitation/emission settings for calcein AM (495/515 nm) and ethidium homodimer (495/635 nm). At least three independent experiments were analysed for each condition.

2.9. Statistics

Statistical analysis was performed with IBM SPSS software. Data were expressed as mean ± standard deviation and differences were considered significant when $p<0.05$. Student's t-test to detect significant differences between two groups and ANOVA to multiple comparisons was used. Depending on the results of the Levene test of homogeneity of variances, Bonferroni or Tamhane post-hoc test was applied. For non-normally distributed data, Mann-Whitney nonparametric analysis was applied.

3. Results and discussion

3D-bioprinting is generally considered to be a powerful manufacture technique in TE since it allows the fabrication of scaffolds and artificial tissues in a controlled way.[2,11] Nonetheless, when introducing cells on supportive inks, the sterilisation assurance must be taken into account. Thus, three different sterilisation techniques, short and long cycle autoclaving, β-radiation and γ-radiation, on the NC-Alg and NC-Alg-HA cell-free bioinks were evaluated.

First, the sterility of all cell-free bioinks was studied according to the European Pharmacopeia to ensure no contamination. After carrying out the sterilisation methods,

bioinks were incubated in the corresponding media for 14 days. Bioinks observation resulted in no turbidity detection (data not shown), which proved that NC-Alg and NC-Alg-HA bioinks were completely free of contaminating microorganisms after sterilisation by autoclaving with short and long procedures, β-radiation and γ-radiation. All negative control tubes were negative after the required incubation period.

The lack of contamination indicated that any of these methods are useful for NC-Alg based bioinks sterilisation. However, these processes may imply important physicochemical changes on bioinks characteristics resulting in bioprinting failure.[11] For this reason, the first objective was to study whatever these sterilisation methods provoke relevant modifications on the characteristics that are of key importance for the printing process, such as the rheological and the physicochemical features.

3.1. Effect of different sterilisation methods on NC-Alg-based bioinks

3.1.1. Rheological properties

Bioprinting through the extrusion procedure requires the study of some fundamental properties of the bioinks such as their rheological characteristics. The rheological characterization of the NC-Alg based bioinks was studied by steady flow and oscillatory shear measurements before and after sterilisation.

Before sterilisation, NC-Alg and NC-Alg-HA bioinks showed shear thinning behaviour with a decrease in viscosity under shear strain. In addition, when shear rate values decreased, viscosity values return to the initial levels showing a thixotropic behaviour (Figure 2). These properties are extremely useful for extrusion-based bioprinting because the deposition of the bioink is facilitated when it is extruded through a nozzle since the applied pressure decreases the bioink viscosity. Just after exiting the nozzle, the shear stress is removed and bioink viscosity increases sharply due to thixotropy.[42] Interestingly, the addition of HA to the NC-Alg bioink showed an enhancement on the viscosity values, achieving around 500 Pa.s at 0.1 s^{-1} shear rate (Figure 2B), whereas without HA only a value of 400 Pa.s was achieved (Figure 2A). This suggests that the addition of HA improves the NC-Alg bioink rheological properties and, therefore, its printability by extrusion.
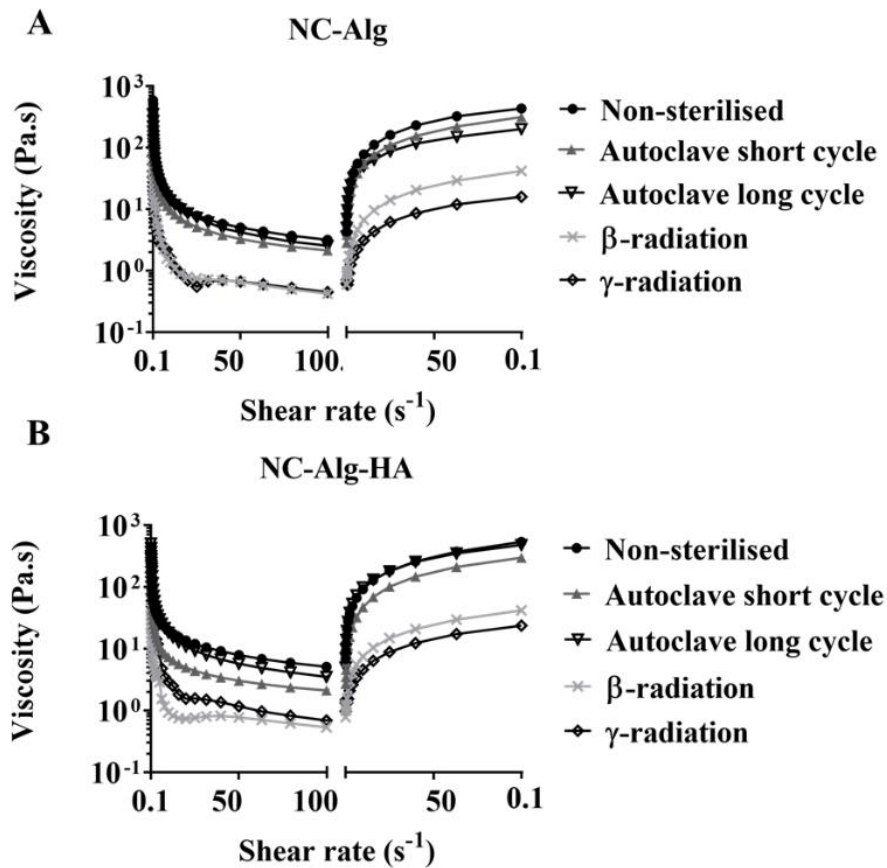
Figure 2. Effect of sterilisation methods on NC-Alg (A) and NC-Alg-HA (B) bioinks rheological properties. Viscosity values were measured before and after sterilisation by short and long cycle autoclaving, β-radiation and γ-radiation.

The viscosity increase due to the incorporation of HA has been previously reported in the literature. One study indicated an improvement of the shear thinning property by increasing the HA content up to 50 % on a gelatin-based bioink.[43] Moreover, higher viscosity values improve the printing fidelity, as the formation of filaments is better in comparison with low viscosity bioinks, which spread out on the bioprinting plate when extruded.[42] Therefore, our bioinks were expected to be easily bioprinted by the extrusion 3D bioprinter.

In Figure 2 it can also be observed the effect of the proposed sterilisation methods. Although all samples maintained the thixotropic property, there were remarkable differences among the effects of the sterilisation procedures.

Short and long cycle autoclaved bioinks showed similar viscosity values compared to the non-sterilised bioinks, which suggests that these sterilised bioinks would show good printable properties. Nonetheless, an important modification in this parameter was

observed on both bioinks after the ionising radiation treatments. Sterilisation by γ-radiation consists of the disruption of the DNA double helix of microorganisms due to the high doses of free radicals that are formed after electron excitation. Similar to γ-radiation, β-radiation damages the DNA of microorganisms but, it does have lower penetration capacity than γ-radiation and requires higher dose rates.[15,44]. In this study, the same dose of 25 kGy was applied for both radiation procedures. The rheological study showed a sharp decrease in viscosity for both bioinks. In fact, although ionising radiations have been widely used as sterilisation methods in several biomedical fields, their destructive effects are known.[11,45] When comparing both radiation types, studies in the literature are inconclusive; one study showed that after applying β and γ-radiations on PLGA spheres, radicals were formed due to polymer destruction, independently of the radiation type.[46,47] However, another study on scaffolds fabricated with l-lactide (LLA), ε-caprolactone (CL) and 1.5-dioxepane-2-one (DXO) polymers, indicated that γ-radiation caused more important damages on the polymers.[16] Therefore, the effects of radiation-based sterilisation techniques on different materials depends not only on the type of radiation but also on the bioinks composition. Regarding this fact, it has been published that when these two radiation types were applied on hydroxypropyl-methyl cellulose (HPMC) and gelatin hydrogels, the viscosity reduction was more evident on HPMC-based gels, probably because its polymer chains are longer compared to gelatin.[43] In our case, γ-radiation provoked a considerable viscosity decrease in our two bioinks, which is in accordance with other studies reporting that γ-radiation causes chain scission on cellulose derived polymers[48] and Alg-based bioinks.[11]

Comparing NC-Alg and NC-Alg-HA bioinks, it was observed that the addition of HA on the NC-Alg mixture appeared to protect this bioink from the harmful effects of γ-radiation (Figure 2B). However, the NC-Alg-HA bioink still showed a lower viscosity in comparison with its non-sterilised control bioink. In fact, modifications in the physical and chemical nature of the polymeric HA have also been reported after radiation.[49] Moreover, degradation of polysaccharides by the cleavage of the glycosidic bonds can occur after ionising radiations.[11,48] The chain scission results in molecular weight reduction, which is reflected on viscosity.[42]

Afterwards, in order to study bioinks viscoelastic properties, frequency sweep measurements were performed. Figure 3A shows that in both non-sterilised bioinks the

storage modulus G' and loss modulus G'' increased under frequency. As G' was higher than G'', both bioinks showed an elastic solid-like behaviour. The loss modulus G'' was higher when HA was added (at 100 Hz, NC-Alg G'' was 808 Pa and with HA 1506 Pa), whereas the storage modulus G' was similar for both bioinks (NC-Alg was 2200 Pa and NC-Alg-HA was 2295 Pa). Therefore, the incorporation of HA in the NC-Alg bioink was able to enhance the viscous modulus.
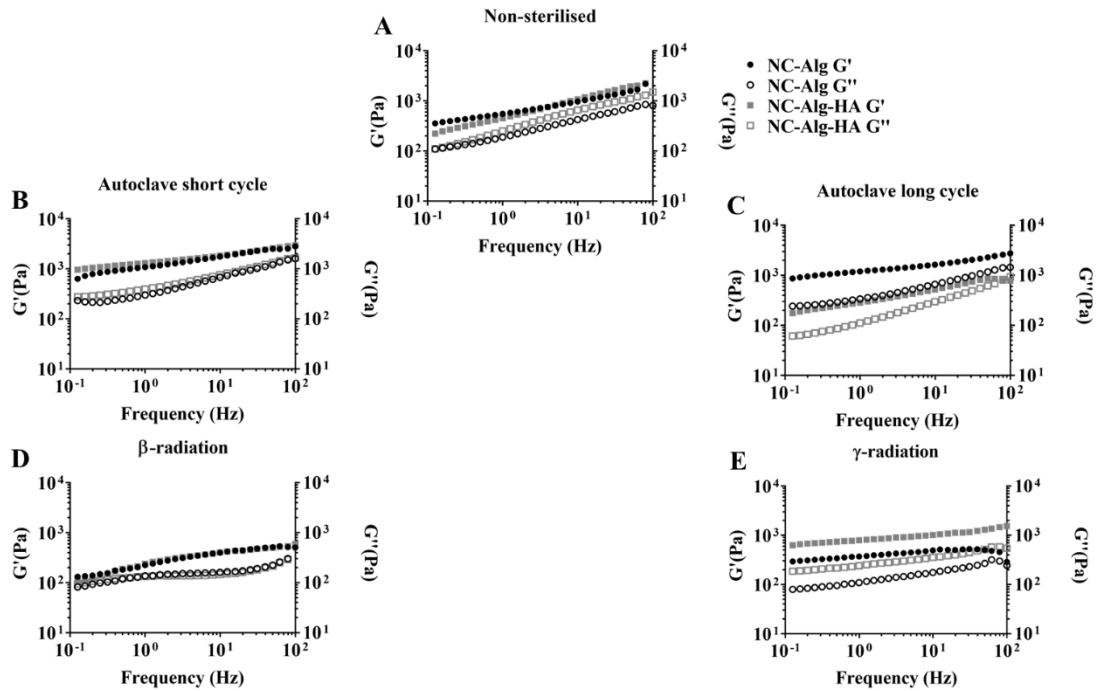

Figure 3. Effect of sterilisation methods on NC-Alg and NC-Alg-HA bioinks frequency sweep measurements and viscoelasticity modules (G' and G''). A) Non-sterilised B) Short cycle autoclave; C) Long cycle autoclave; D) β-radiation; E) γ-radiation.

Next the sterilisation effect on viscoelasticity was evaluated. Independently of the applied sterilisation technique, both bioinks maintained the elastic solid-like behaviour. However, changes on G' and G'' values were observed. As Figure 3B shows, after short cycle autoclaving procedure, both bioinks showed similar G' and G'' values, but a slight increase in viscoelasticity was observed when compared to non-sterilised bioinks (at 100 Hz, sterile NC-Alg G'' was 1497 Pa and NC-Alg- HA was 1655 Pa). In contrast, after long cycle autoclaving, the NC-Alg bioink showed higher G' and G'' values compared to the HA bioink (at 100 Hz, sterile NC-Alg G' and G'' were 2592 Pa and 1416 Pa respectively, and with HA were 853 Pa and 826 Pa respectively) (Figure 3C).

In addition, viscoelasticity values of the NC-Alg bioink were slightly higher in comparison with the non-sterilised sample. In contrast, the HA containing bioink showed a reduction on G' and G'' values after sterilisation. This suggests that after the application of a long cycle autoclaving process, HA was probably damaged resulting in a lower viscous modulus value (G''). Importantly, it has been described that the viscosity of 0.5 -2 % HA aqueous solutions decreases when the temperature increases due to hydrogen bond breakage, resulting in weakening of the entanglement couplings. [50,51]

After the application of β-radiation (Figure 3D), viscoelasticity properties of both bioinks decreased comparing to the non-sterilised samples (at 100 Hz, NC-Alg sterile bioink G' and G'' were 504 Pa and 224 Pa, respectively and NC-Alg-HA were 598 Pa and 210 Pa, respectively). This sharp reduction on viscoelasticity properties of both bioinks might be related with the molecular weight loss of cellulose, which has been already reported after β-radiation.[52] After γ-radiation (Figure 3E) differences between the two bioinks were detected; While the NC-Alg bioink showed a reduction on viscoelasticity in comparison to the non-sterilised sample, the NC-Alg-HA bioink demonstrated higher G' and G'' values. This suggests that the NC-Alg bioink G' and G'' values were modified after the application of both radiation types, but the NC-Alg-HA bioink only was damaged by β-rays. This may be explained by the overheating that β-rays may cause.[44]

3.1.2. Physicochemical properties

Next, macroscopic characteristics, osmolality and pH of NC-Alg and NC-Alg-HA bioinks were studied before and after sterilisation. Between the NC-Alg and the NC-Alg-HA bioinks there were not significant differences regarding their physical appearance. Both were white and homogenous. After applying any of the sterilisation techniques evaluated, bioinks maintained their physiochemical characteristics (supplementary material).

The osmolality study indicated no significant differences between both non-sterilised bioinks (0.0653 ± 0.0005 Osmol/kg for NC-Alg and 0.0883 ± 0.0006 Osmol/kg for NC-Alg-HA) (Figure 4A). NC-Alg-HA bioink demonstrated higher osmolality values which suggests more physiological behaviour. Hyaluronic is a component of extracellular matrix in many tissues and, as much as the other glycosaminoglycans, may increase the

osmolality of solutions[53]. Nonetheless, since physiological osmolality values are around 0.28 Osmol/kg, both bioinks showed to be hypoosmotic. However, no negative effects have been detected on cell behaviour due to cell embedded scaffolds culture is carried out inside abundant culture media. Subsequently osmolality was measured again in order to know if the sterilisation methods had any effect on this parameter. After both autoclaving procedures, NC-Alg bioink showed an increase in osmolality ($p < 0.001$). Similarly, these procedures enhanced the osmolality values of the HA-containing bioink (short cycle ($p < 0.001$) and long cycle ($p < 0.01$)). In contrast, after β-radiation only the NC-Alg bioink osmolality increased significantly ($p < 0.001$). Importantly, the effect was more accentuated after γ-radiation. In this case, osmolality values increased significantly on both bioinks ($p < 0.001$). It is known that degradation of biopolymers and polysaccharides could occur after heating or radiation treatments inducing molecular weight reductions. The occurred chain scission might increase the presence of radicals and osmotically active solutes in the media.[44,46] Therefore, it can be hypothesized that biopolymer structural changes occurring because of the sterilisation processes would increase bioinks osmolality.
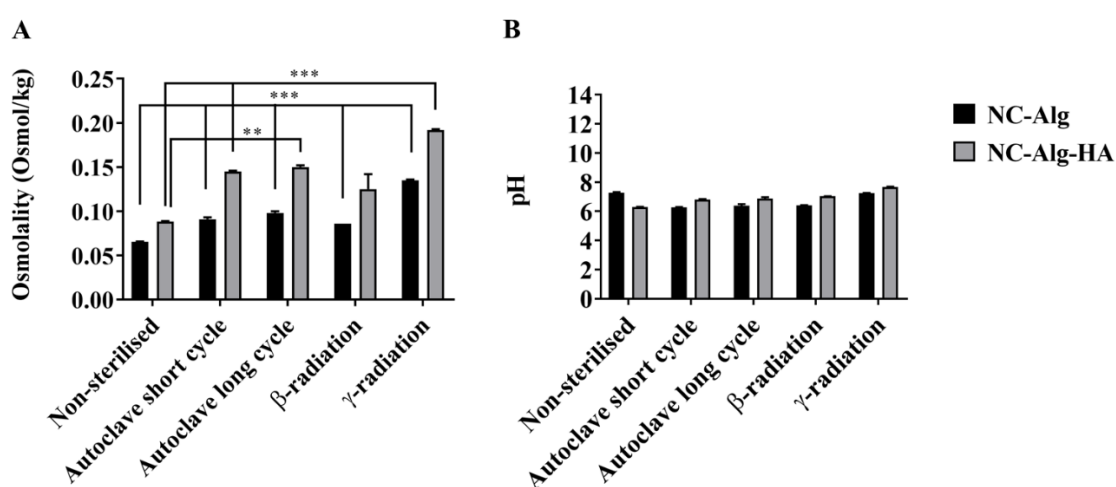

Figure 4. Effect of sterilisation methods on NC-Alg and NC-Alg-HA bioinks A) Osmolality and B) pH. Values represent mean ± SD. ***: $p < 0.001$; **: $p < 0.01$.

On the other hand, both non-sterilised bioinks showed pH values close to the physiological ones (7.29 ± 0.04 for NC-Alg and 6.28 ± 0.03 for NC-Alg-HA), and after sterilisation, the pH values were maintained without significant variations, as it is shown in Figure 4B.

3.2. Printability determination of bioinks

Once the NC-Alg and NC-Alg-HA bioinks had been characterised and the effects of the different methods of sterilisation had been evaluated, printability evaluation was required. Scaffolds were fabricated by the extrusion bioprinter following the parameters described before (section 2.6). The rheological studies in which the NC-Alg-HA bioink showed higher viscosity than the NC-Alg bioink resulted in the need of applying a higher pressure on bioprinting in order to be able to extrude the bioink through the nozzle (from 20 kPa of NC-Alg to 26 kPa of NC-Alg-HA). In addition, printability was evaluated after sterilisation.

After autoclaving (short and long cycle), similar bioprinting parameters were maintained. As an example, it can be observed in Figure 5A1 that the macroscopic appearance complied accurately with the computer design of the scaffold. Figure 5A2 shows the scaffold obtained after sterilising the NC-Alg-HA bioink by short cycle autoclaving. The printing results, together with rheological properties, indicated that bioinks sterilised through autoclave were adequate for extrusion printing. In contrast, when radiated bioinks were used, extrusion led to wide viscous strands which required lower extrusion pressures and printing speed. The obtained scaffolds revealed lack of shape fidelity (supplementary material). These findings are supported by the accentuated decrease in viscosity showed in the rheological study. As discussed before, main-chain scission and cross-linking damages caused by ionising radiations avoided the bioprinting of properly defined scaffolds and, therefore, the scaffolds were unable to maintain their shape.
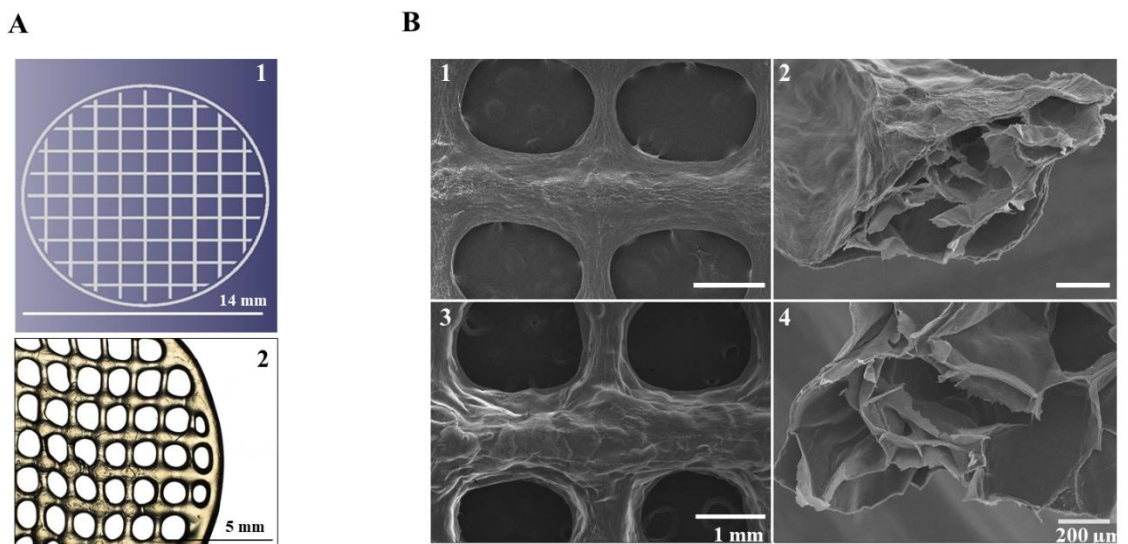
Figure 5. Morphological characterization. A) Computer assisted design of the scaffold (1) vs bioprinted scaffold after autoclaving the NC-Alg-HA bioink by short cycle. Scale bar in 1: 14 mm and in 2: 5 mm (2). B) Representative scanning electron microscopy images of NC-Alg (1-2) and NC-Alg-HA (3-4) scaffolds. Scale bar in 1 and 3: 1 mm; in 2 and 4: 200 μm.

According to the rheological studies and the analysis of the physicochemical properties of the two cell-free bioinks as well as the printability study, it could be concluded that the sterilisation by using the short cycle autoclaving technique had the lowest effect on the original characteristics of the bioinks. Therefore, it was elected as the best option for sterilising both the NC-Alg and the NC-Alg-HA bioinks. However, prior to the introduction of cells in order to analyse the application of these scaffolds for TE, other aspects such as the 3D printed scaffolds characterization were evaluated.

3.3. Morphological characterization of printed scaffolds

3.3.1. Scanning electron microscopy (SEM)

NC-Alg and NC-Alg-HA scaffolds were analysed by SEM in order to observe their external and internal structure that has been recognised as important factors for defining cellular behaviour.[39] The superficial structure showed that scaffolds with HA presented more fibrous structures (Figure 5B, 3). In addition, the inner part of the scaffolds were observed by making crosscuts. A porous internal structure with channel-like arrangement was found in both scaffolds, which suggests that proper oxygen and nutrients transport can be ensured for achieving high cell viability and proliferation.

3.3.2. Surface and architectural structure study

In order to attain a more in-depth study of the architectural structures of both scaffolds, an optical profilometer technique was used. No reference has been found to this technique being used for studying printed scaffolds. Figure 6A shows representative axonometric 3D images of the measurements carried out in the bioprinted scaffolds. Architectural differences can be observed between NC-Alg and NC-Alg-HA scaffolds. In fact, the NC-Alg-HA grid morphology is less rounded compared to the NC-Alg bioink, which generated more oblong shaped grids. In addition, the NC-Alg-HA scaffolds presented a significantly higher amount of deposited material compared to the

NC-Alg scaffolds (3.51 ± 0.55 mm^3 NC-Alg scaffolds versus 7.53 ± 2.10 mm^3 NC-Alg-HA scaffolds) (Figure 6B). However, both printed scaffolds presented a similar grid area and aspect ratio as Figure 6C shows. The higher amount of deposited material in NC-Alg-HA scaffolds could be explained by the rheological and printability studies in which the NC-Alg-HA bioink showed higher viscosity than the NC-Alg bioink. This enhancement in viscosity resulted in the need for the application of a higher pressure on the bioprinting technique in order to be able to extrude the bioink through the nozzle. This increment in pressure may involve a higher amount of HA-containing bioink being extruded and, therefore, the amount of material deposited in the scaffolds.
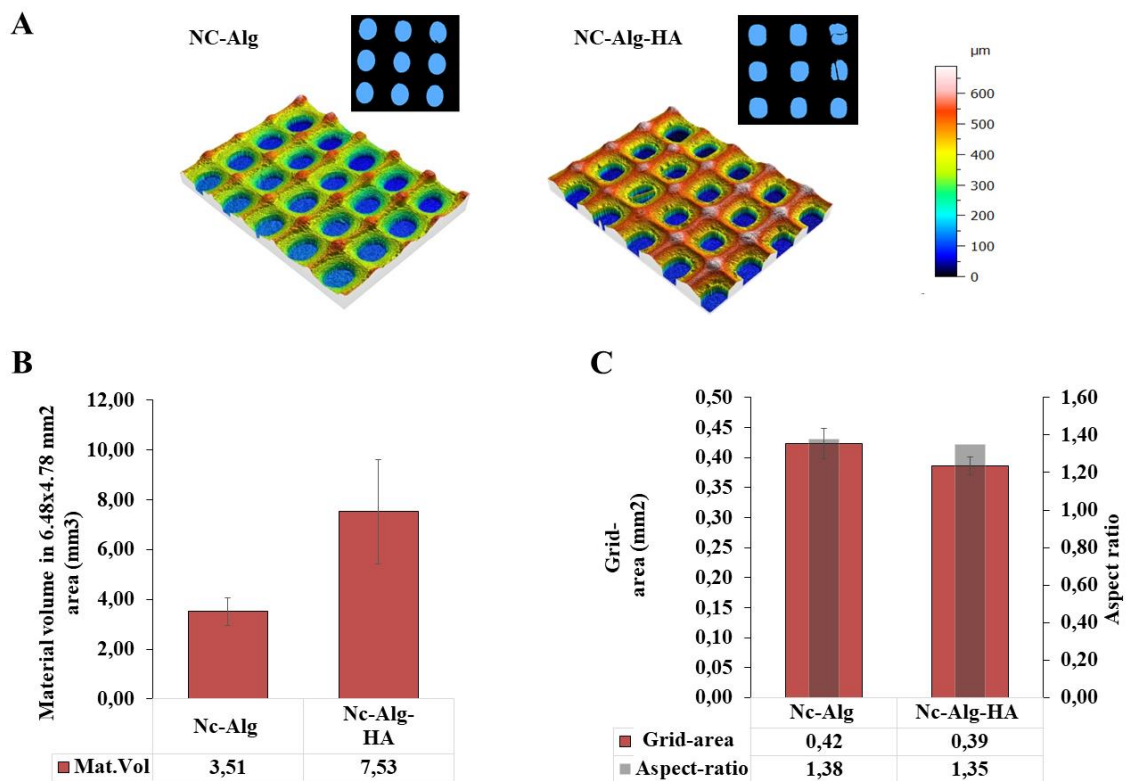

Figure 6. Surface and architectural structure study of NC-Alg and NC-Alg-HA 3D printed scaffolds. A) Representative images of the topology measurements and binarized areas of the printed scaffolds. B) Deposited material volume analysis. C) Grid area and aspect ratio computed from binarized data analysis. Values represent mean ± SD.

This phenomenon was also shown in Figure 7A-B in which NC-Alg-HA printed structures resulted in significantly thicker scaffolds on Y axis (p<0.01) compared to the

NC-Alg scaffolds (NC-Alg scaffolds, in Y direction 432 ± 30 µm; NC-Alg-HA scaffolds, 552 ± 24 µm). NC-Alg-HA scaffolds also resulted in a significantly greater height on two axis (p<0.01) (NC-Alg scaffold, in X direction 345 ± 30 µm and in Y direction 215 ± 28 µm; NC-Alg-HA scaffolds, in X direction 549 ± 63 µm and in Y direction 476 ± 29 µm) (Figure 7A-B). The strut shape also varied according to the direction for both bioinks, presenting a smaller height and thickness of the struts in the Y direction. However, despite the fact that NC-Alg-HA bioink was extruded in a higher quantity, the obtained scaffolds did not show loss of structure fidelity. In fact, both scaffolds grid areas were similar.
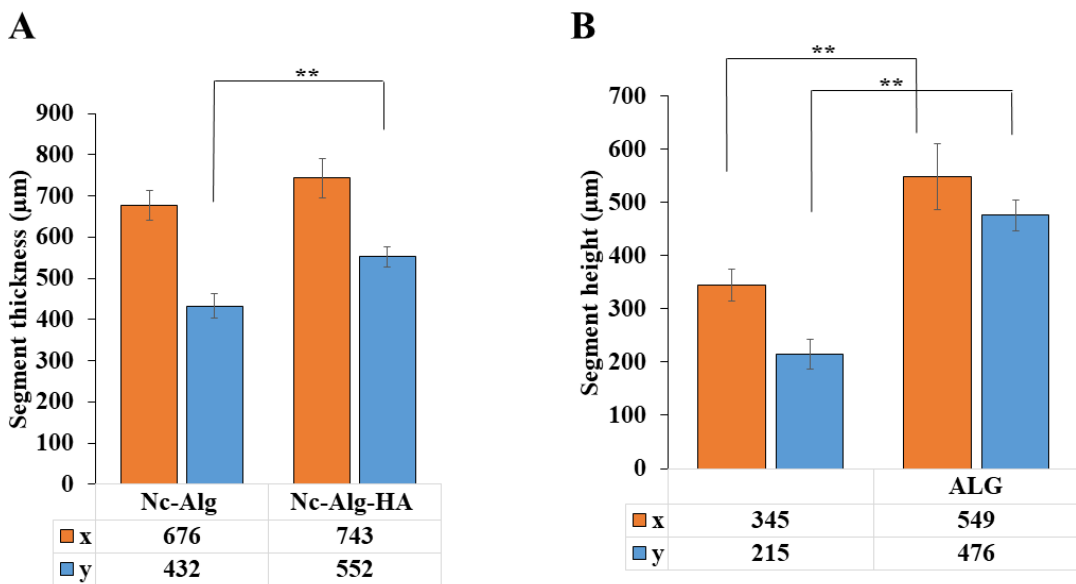

A

	Nc-Alg	Nc-Alg-HA
x	676	743
y	432	552

B

		ALG
x	345	549
y	215	476

Figure 7. Surface and architectural structure study on NC-Alg and NC-Alg-HA scaffolds. Analysis of the strut architecture of the bioprinted scaffolds in terms of thickness (A) and height (B). Values represent mean ± SD. **: p<0.01.

Regarding the surface topography, it has been reported that it affects cells differentiation and tissue formation, such as bone.[54] NC-Alg printed scaffolds presented greater height characteristics (S_q, Figure 8A). However, the NC-Alg-HA bioprinted scaffolds reported a superior developed surface area (S_{dr} Figure 8B). The biggest topographical difference was observed in terms of lateral characteristics (S_{al} Figure 8C). The bigger S_{al} parameter value on NC-Alg scaffolds indicates in Figure 8D that the NC-Alg surface was dominated by larger wavelength components (texture presents bigger spacing) while NC-Alg-HA printed scaffolds presented a less spaced

texture. However, there were no significant differences between both scaffolds, and the implication of these parameters on cells differentiation should be analysed in future studies.
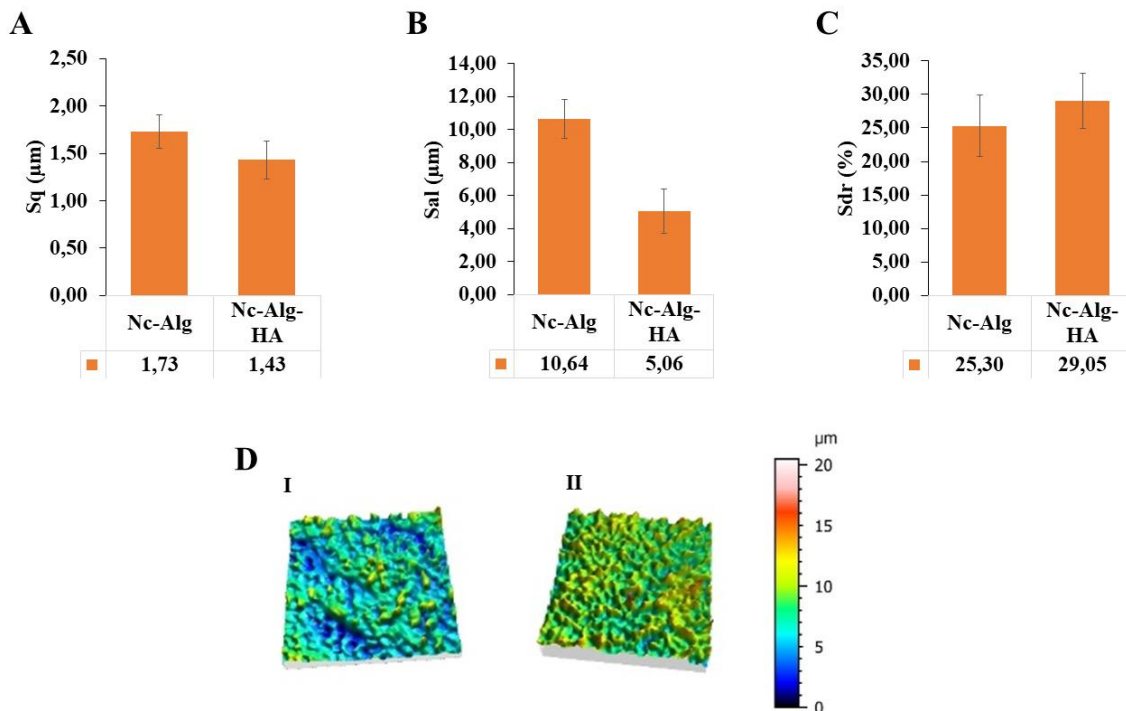

Figure 8 Surface and architectural structure study on NC-Alg and NC-Alg-HA scaffolds. A-C) 3D topographical parameters describing height (S_q), lateral (S_{sal}) and hybrid (S_{dr}) characteristics of the scaffolds. Values represent mean ± SD. D) Representative axonometric projections of the topographical measurements of the NC-Alg (I) and NC-Alg-HA (II) scaffolds.

3.4. Swelling determination and scaffolds degradation analysis

Before introducing cells into the NC-Alg and NC-Alg-HA bioinks for printing the 3D scaffolds, swelling and degradation analysis of cell-free structures was performed.

The evaluation of swelling is important since it relates to substance exchange when used for biomedical applications as well as many other properties such as flexibility and mechanical properties.[55,56] In our study, water uptake by both printed scaffolds

increased over the time until they reached the equilibrium with NC-Alg scaffolds reached it within 6 to 8 hours, whereas the NC-Alg-HA scaffolds reached this steadiness earlier, within 3 to 4 hours (Figure 9A). Our results indicated fast swelling properties, which may be caused by the hydrophilicity of NC, Alg and HA. Some studies have reported that high elasticity values resulted in faster water uptake.[57] This may explain why the NC-Alg-HA scaffolds reached the equilibrium faster than the NC-Alg scaffolds.

On the other hand, although no statistically significant differences were detected, the NC-Alg scaffolds water uptake was slightly higher (NC-Alg scaffolds swelling 95.61 ± 0.84 % versus 94.34 ± 0.01 % in NC-Alg-HA scaffolds). As it has been reported, dense bioinks swelling values decrease due to their dense inner structure.[55] Thus, this may explain why the HA-containing scaffolds absorbed less water, as this bioink had higher viscosity than the NC-Alg.
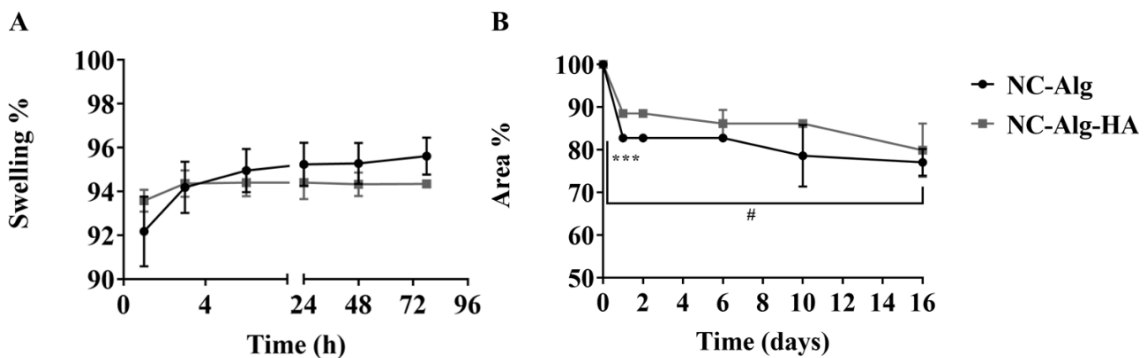

Figure 9. NC-Alg and NC-Alg-HA printed scaffolds swelling determination (A) and degradation rate (B). Values represent mean ± SD. ***: p<0.001, comparison between both scaffolds. #: p<0.05, comparison between days in the same scaffold.

Degradation studies are essential in the evaluation of scaffolds behaviour and its implications on cells studies, such as differentiation and *in vivo* tissue formation.[58,59] Furthermore, a desirable feature in regenerative medicine would be the synchronization of scaffold degradation with the replacement by natural tissue produced from cells.[60] As Figure 9B shows, NC-Alg and NC-Alg-HA scaffolds decreased their area during the first 24 hours this reduction being more accentuated for the scaffolds without HA

(p<0.001) (NC-Alg 17.21 ± 0.15 % area reduction versus 11.50 ± 0.36 % in NC-Alg-HA scaffolds). The degradation rate was more progressive during the remainder of the assay. At the final point (day 16th), the total area reduction in the NC-Alg scaffolds was 22.94 ± 3.12 % versus 20.10 ± 6.25 % in the NC-Alg-HA scaffolds. It is noteworthy that the water content uptake ability of hydrophilic scaffolds causes major degradation rates because of the decreasing the density of crosslinking and crystallization, as has been reported in Alg based scaffolds.[61]

As the swelling assay demonstrated, both scaffolds had high water uptake capacity; nevertheless, the addition of HA prevented from a faster degradation of scaffolds during the first hours after printing. Importantly, degradation rate is related with the material characteristics and crosslinking procedure. Thus, highly crosslinked scaffolds showed slow degradation rates *in vitro* which made cell proliferation and protein release difficult to achieve.[62] On the other hand, fast degradative scaffolds have been demonstrated to be inefficient in tissue regeneration.[60] Our both scaffolds showed a controlled degradation values over the time, however, modelling of degradation processes *in vivo* may be needed in order to understand how it repercuss in tissue regeneration.

3.5. Biological analysis

3.5.1. Cytotoxicity analysis of the bioinks

Once bioinks and scaffolds were characterised, cytotoxicity evaluation was needed prior to the introduction of cells into inks. To analyse any potential harmful effects of NC-Alg based inks on cell viability, the adhesion, direct contact and indirect contact cytotoxicity tests were performed according to ISO 10993-5-2009[41] (Figure 10).

In the adhesion assay, both bioinks showed similar cell viability (NC-Alg bioink 98.55 ± 20.30 % and NC-Alg-HA bioink 99.34 ± 12.20 %). Similarly, the direct contact assay showed that cell viability was above 70 %, which indicates that both bioinks have no potential harmful effects on L929 cells (NC-Alg 88.53 ± 32.91 % and NC-Alg-HA 74.12 ± 31.62 %). Importantly, the addition of HA on the NC-Alg base bioink resulted in a significantly higher cell viability (p<0.001). HA constitutes the basic component of extracellular matrix in some tissues and it has been described for being involved in a wide variety of biological procedures, such as cell signalling mediation, regulation of

cell adhesion and proliferation. [63] This assay was performed by adding conditioned DMEM that previously had been in contact with the bioink, onto seeded L929 cells. It may be that the presence of HA on the media enhanced cell viability and proliferation. Another study reports that cell viability increases by adding HA supplemented media as it decreases mitochondrial DNA damage while enhancing DNA repair capacity, cell viability, preservation of ATP levels, and amelioration of apoptosis.[63]
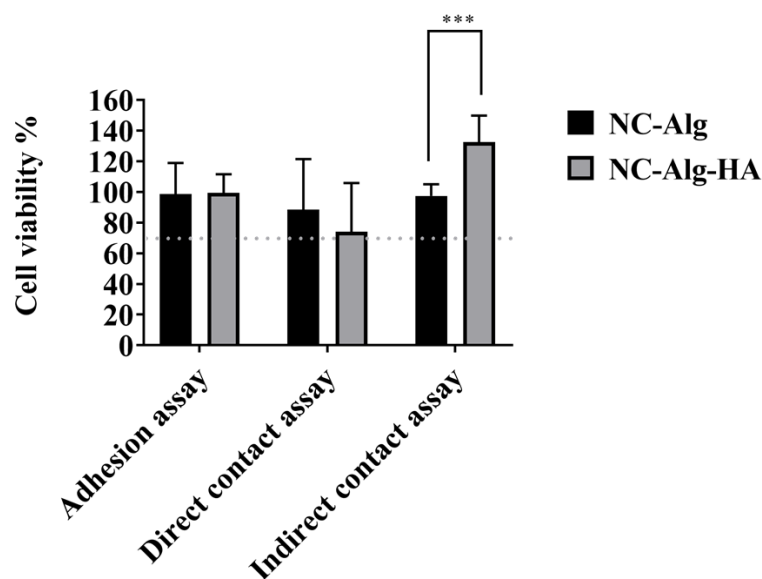

Figure 10. Cytotoxicity analysis of NC-Alg and NC-Alg-HA bioinks in adhesion, direct contact and indirect contact assays. Values represent mean ± SD. ***: p<0.001.

3.5.2. Viability and metabolic activity of D1-MSCs in the bioprinted scaffolds

Once the non-toxicity had been ensured different densities of previously sterilised – by short cycle autoclave - murine D1-MSCs were mixed. MSCs are widely applied in tissue regenerative fields since they characterize by their potential to differentiate into a variety of cell types, including osteoblasts, chondrocytes, adipocytes and myocytes.[64] D1 cell line was previously reported to have the capacity to differentiate spontaneously into osteoblasts, and in adipocytes when using pro-adipogenic agents.[32,64] After an analysis of the available literature no unique adequate cell density to seed was found; in

fact, in other studies a wide range of densities have been used. Thus, in this study, cell densities between 1×10^6 and 5×10^6 cell/mL were selected. However, the lowest density of 1×10^6 cell/mL showed very low viability values and proliferation rates (supplementary material) and therefore, the assays were continued with 2.5×10^6 and 5×10^6 cell/mL. Then, circular grid-like constructs of 14 mm diameter and 4 layers in height were bioprinted through a 27 G nozzle by the extruder bioprinter. In order to evaluate the feasibility of NC-Alg and NC-Alg-HA constructs as adequate 3D structures to maintain cell survival, the metabolic activity as well as viability of embedded cells were determined at several time points.

As Figure 11 shows, cells were alive in the NC-Alg scaffolds as well as in those containing HA at both cell densities after the bioprinting process. Several studies have previously indicated that cell viability may decrease after extrusion-based bioprinting procedures due to the huge stress that cells might suffer during the process.[56] In this study, however, biological assays demonstrated high cell survival in both 3D constructs after the bioprinting process, which suggests that the shear thinning behaviour of bioinks may be acting as a protection factor for the cells.[30]

The metabolic activity of these cells was assayed over 3 weeks (Figure 11A). As expected, the metabolic activity was higher when a higher cell density was added to the bioink before 3D-bioprinting. Over time, apart from a reduction on the arbitrary fluorescence units (RFU) on day 7 for the 2.5×10^6 cell/mL density in the NC-Alg scaffolds, the measured metabolic activity was stable in both scaffolds at both cell densities. Now, when a comparison is made, the HA seems to protect the cells during the first days or the first week. This effect was more prominent for the lower cell density condition (day 1, $p < 0.001$ and day 7, $p < 0.01$). The significantly higher cell metabolism in the HA containing scaffolds may be related to the improvement of the rheological properties of the bioink when HA was added. Besides, the positive effects of HA on cells have been widely described. It has been reported that the addition of HA on Alg hydrogels promotes MSCs viability and functionality.[31] Other studies have shown that HA containing bioinks improve cell differentiation of hMSCs.[65] In fact, stem cells receive signals from the environment; therefore, HA, as an extracellular matrix component, significantly influences all these biological responses.
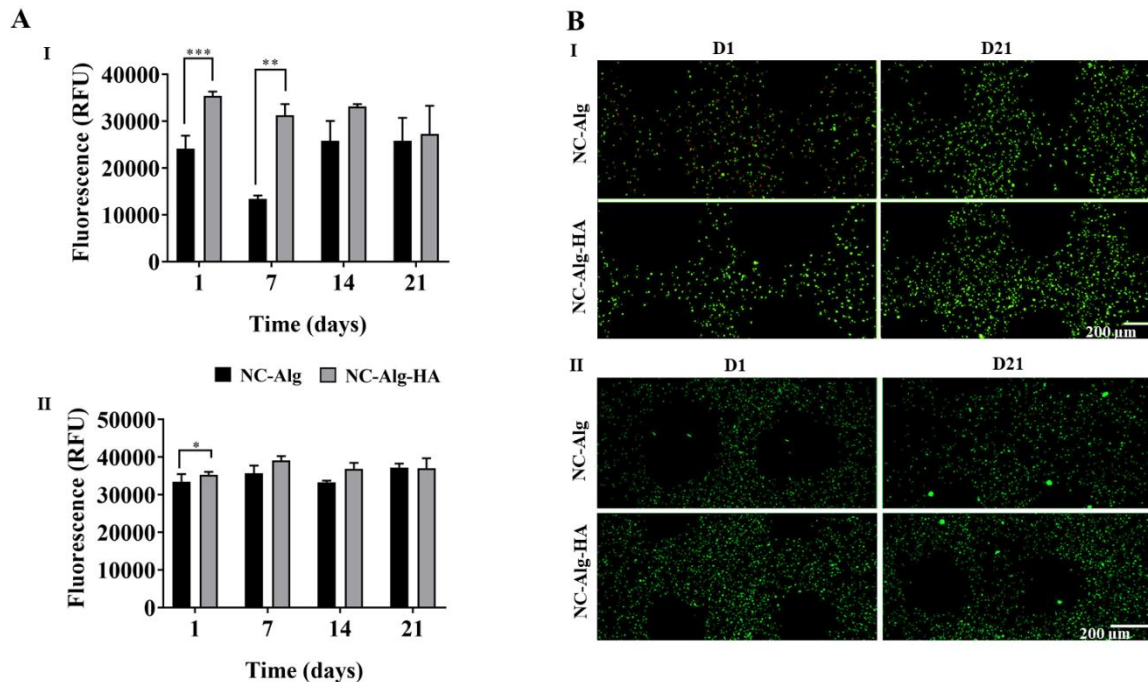
Figure 11. Cell viability studies. A) Metabolic activity assay at two different cell densities: I) 2.5×10^6 cell/mL and II) 5×10^6 cell/mL. Values represent mean ± SD. ***: $p < 0.001$; **: $p < 0.01$; *: $p < 0.05$. B) Representative fluorescence micrographs of live/dead stained scaffolds I) 2.5×10^6 cell/mL and II) 5×10^6 cell/mL, showing live (green) and dead (red) cells at day 1 and 21 after bioprinting. Scale bar 200 μm.

The live/dead staining was carried out for 21 days. Figure 11B corroborated cell survival and shows that embedded cells were homogeneously distributed in bioprinted scaffolds. Then, L/D pictures were analysed using Image J software in order to show the percentage between cells alive (in green) and dead (in read). At D1 after bioprinting, results showed that cell viability was higher on scaffolds containing HA at 2.5×10^6 cell/mL density (NC-Alg scaffolds 80 ± 23 % and the HA containing scaffolds 90 ± 12 %). This tendency was repeated at 5×10^6 cell/mL density, being on NC-Alg scaffolds 72 ± 6 % and on NC-Alg-HA scaffolds 95 ± 7 %. Furthermore, at D21 after bioprinting NC-Alg-HA scaffolds showed higher cells alive than NC-Alg scaffolds too. This corroborates the protective function of HA that has been previously discussed. In addition, when comparing the two cell densities, cells aggregates were found at 5×10^6 cell/mL density on both constructs at the end of the assay. As one study reported, cell aggregates may be necessary to induce the differentiation of MSCs into chondrocytes in

3D cultures,[66] which suggests that NC-Alg based scaffolds may become a feasible tissue engineering approach for cartilage regeneration at high cell densities.

4. Conclusions

First, this study was focused on sterilisation of bioinks for 3D-bioprinting. Since UV has been found to be ineffective[17] and ethylene oxide resulted in cancerous chemical residue,[15] a study was carried out the most commonly used sterilisation techniques in the biomedical field: autoclave by short and long procedures, β-radiation and γ-radiation. All techniques were effective ensuring the sterility of NC-Alg and NC-Alg-HA cell-free bioinks. Nevertheless, based on fundamental properties for bioinks such as rheology, physicochemical and printability, short cycle autoclaving was found to be the best sterilisation technique for NC-Alg based bioinks. Moreover, the addition of HA to the bioink resulted in the improvement of rheological properties which had repercussions on the printing procedure, as well as in bioink physiological behaviour.

Further, an evaluation of the bioprinted scaffolds to be used for tissue engineering was also conducted. The structure, swelling and degradation of both scaffolds were also evaluated. In addition, the biological studies with D1-MSCs-loaded constructs showed better results in HA-containing matrices, which indicates that NC-Alg-HA mixtures are an excellent bioink for the development of 3D bioprinted scaffolds for TE and regenerative medicine of cartilage tissue.

Acknowledgements

Formulation Unit (U10) of the CIBER in Bioengineering, Biomaterials & Nanomedicine (CIBER-BBN) at the University of Basque Country (UPV/EHU).

5. References

[1] S Derakhshanfar, R Mbeleck, K Xu, X Zhang, W Zhong, M Xing. 3D bioprinting for biomedical devices and tissue engineering: A review of recent trends and advances, Bioactive Materials. 3 (2018) 144-156.

[2] D Nguyen, DA Hägg, A Forsman, J Ekholm, P Nimkingratana, C Brantsing, et al. Cartilage Tissue Engineering by the 3D Bioprinting of iPS Cells in a Nanocellulose/Alginate Bioink, Scientific reports. 7 (2017) 658-10.

[3] Z Xie, M Gao, AO Lobo, TJ Webster. 3D Bioprinting in Tissue Engineering for Medical Applications: The Classic and the Hybrid, Polymers. 12 (2020) 1717.

[4] J Li, L He, C Zhou, Y Zhou, Y Bai, FY Lee, et al. 3D printing for regenerative medicine: From bench to bedside, MRS bulletin. 40 (2015) 145-154.

[5] YP Singh, A Bandyopadhyay, BB Mandal. 3D Bioprinting Using Cross-Linker-Free Silk–Gelatin Bioink for Cartilage Tissue Engineering, ACS applied materials & interfaces. 11 (2019) 33684-33696.

[6] M Varkey, DO Visscher, van Zuijlen, Paul P. M, A Atala, JJ Yoo. Skin bioprinting: the future of burn wound reconstruction? Burns and trauma. 7 (2019) 4.

[7] P He, J Zhao, J Zhang, B Li, Z Gou, M Gou, et al., Bioprinting of skin constructs for wound healing, Trauma. 6 (2018).

[8] M Fuest, GH Yam, JS Mehta, DF Duarte Campos. Prospects and Challenges of Translational Corneal Bioprinting, Bioengineering (Basel). 7 (2020) 71.

[9] S Yoo, O Thabit, EK Kim, H Ide, D Yim, A Dragulescu, et al., 3D printing in medicine of congenital heart diseases, 3D Print Med. 2 (2016).

[10] TK Merceron, M Burt, Y Seol, H Kang, SJ Lee, JJ Yoo, et al., A 3D bioprinted complex structure for engineering the muscle–tendon unit, Biofabrication. 7 (2015).

[11] E Hodder, S Duin, D Kilian, T Ahlfeld, J Seidel, C Nachtigall, et al. Investigating the effect of sterilisation methods on the physical properties and cytocompatibility of methyl cellulose used in combination with alginate for 3D-bioplotting of chondrocytes, J Mater Sci: Mater Med. 30 (2019) 1-16.

[12] R Galante, TJA Pinto, R Colaço, AP Serro, Sterilization of hydrogels for biomedical applications: A review, J. Biomed. Mater. Res. 106 (2017) 2472.

[13] M Di Foggia, U Corda, E Plescia, P Taddei, A Torreggiani, Effects of sterilisation by high-energy radiation on biomedical poly-(e-caprolactone)/hydroxyapatite composites. J Mater Sci: Mater Med. 21 (2010) 1789–1797.

[14] CD O'Connell, C Onofrillo, S Duchi, X Li, Y Zhang, P Tian, et al. Evaluation of sterilisation methods for bio-ink components: gelatin, gelatin methacryloyl, hyaluronic acid and hyaluronic acid methacryloyl, Biofabrication. 11 (2019) 035003.

[15] KA Faraj, KM Brouwer, PJ Geutjes, EM Versteeg, PGP Wismans, JA Deprest, et al. The effect of Ethylene Oxide Sterilisation, Beta Irradiation and Gamma Irradiation on Collagen Fibril-Based Scaffolds, Journal of Tissue Engineering and Regenerative Medicine. 8 (2011) 460-470.

[16] Z Dai, J Ronholm, Y Tian, B Sethi, X Cao, Sterilization techniques for biodegradable scaffolds in tissue engineering applications, Journal of Tissue Engineering. 7 (2016) 2041731416648810.

[17] T Lorson, M Ruopp, A Nadernezhad, J Eiber, U Vogel, T Jungst, et al. Sterilization Methods and Their Influence on Physicochemical Properties and Bioprinting of Alginate as a Bioink Component, ACS omega. 5 (2020) 6481-6486.

[18] L Valot, J Martinez, A Mehdi, G Subra. Chemical insights into bioinks for 3D printing, Chemical Society Reviews. (2019).

[19] A Sheikhi, J Hayashi, J Eichenbaum, M Gutin, N Kuntjoro, D Khorsandi, et al. Recent advances in nanoengineering cellulose for cargo delivery, Journal of Controlled Release. 294 (2019) 53-76.

[20] S Salimi, R Sotudeh-Gharebagh, R Zarghami, SY Chan, KH Yuen. Production of Nanocellulose and Its Applications in Drug Delivery: A Critical Review, ACS sustainable chemistry & engineering. 7 (2019) 15800-15827.

[21] A Sharma, M Thakur, M Bhattacharya, T Mandal, S Goswami. Commercial application of cellulose nano-composites – A review, Biotechnology Reports. 21 (2019) e00316.

[22] A Basu, J Lindh, E Ålander, M Strømme, N Ferraz. On the use of ion-crosslinked nanocellulose hydrogels for wound healing solutions: Physicochemical properties and application-oriented biocompatibility studies, Carbohydrate Polymers. 174 (2017) 299-308.

[23] E Axpe, ML Oyen. Applications of Alginate-Based Bioinks in 3D Bioprinting, International journal of molecular sciences. 17 (2016) 1976.

[24] F Yu, X Han, K Zhang, B Dai, S Shen, X Gao, et al. Evaluation of a polyvinyl alcohol-alginate based hydrogel for precise 3D bioprinting, Journal of Biomedical Materials Research Part A. 106 (2018) 2944-2954.

[25] A Murua, M de Castro, G Orive, RM Hernández, JL Pedraz. In Vitro Characterization and In Vivo Functionality of Erythropoietin-Secreting Cells

Immobilized in Alginate−Poly-l-Lysine−Alginate Microcapsules, Biomacromolecules. 8 (2007) 3302-3307.

[26] K Markstedt, A Mantas, I Tournier, H Martínez Ávila, D Hägg, P Gatenholm. 3D Bioprinting Human Chondrocytes with Nanocellulose–Alginate Bioink for Cartilage Tissue Engineering Applications, Biomacromolecules. 16 (1900) 1489-1496.

[27] E Ruvinov, T Tavor Re´em, F Witte, S Cohen. Articular cartilage regeneration using acellular bioactive affinity-binding alginate hydrogel: A 6-month study in a mini-pig model of osteochondral defects, Journal of orthopaedic translation. 16 (2019) 40-52.

[28] M Rubert, M Alonso-Sande, M Monjo, J Ramis. Evaluation of Alginate and Hyaluronic Acid for Their Use in Bone Tissue Engineering, Biointerphases. 7 (2012) 1-11.

[29] S Ansari, I Diniz, C Chen, T Aghaloo, B Wu, S Shi, et al. Alginate/hyaluronic acid hydrogel delivery system characteristics regulate the differentiation of periodontal ligament stem cells toward chondrogenic lineage, J Mater Sci: Mater Med. 28 (2017) 1-12.

[30] C Antich, J de Vicente, G Jiménez, C Chocarro, E Carrillo, E Montañez, et al. Bio-inspired hydrogel composed of hyaluronic acid and alginate as a potential bioink for 3D bioprinting of articular cartilage engineering constructs, Acta Biomaterialia. 106 (2020) 114-123.

[31] A Cañibano-Hernández, L Saenz del Burgo, A Espona-Noguera, G Orive, RM Hernández, J Ciriza, et al. Alginate Microcapsules Incorporating Hyaluronic Acid Recreate Closer in Vivo Environment for Mesenchymal Stem Cells, Molecular Pharmaceutics. 14 (2017) 2390-2399.

[32] A Cañibano-Hernández, L Saenz del Burgo, A Espona-Noguera, G Orive, RM Hernández, J Ciriza, et al. Hyaluronic Acid Promotes Differentiation of Mesenchymal Stem Cells from Different Sources toward Pancreatic Progenitors within Three-Dimensional Alginate Matrixes, Molecular Pharmaceutics. 16 (2019) 834-845.

[33] E López-Ruiz, G Jiménez, L Álvarez de Cienfuegos, C Antic, R Sabata, JA Marcha, et al. Advances of hyaluronic acid in stem cell therapy and tissue engineering, including current clinical trials, European cells & materials. 37 (2019) 186-213.

[34] J Leppiniemi, P Lahtinen, A Paajanen, R Mahlberg, S Metsä-Kortelainen, T Pinomaa, et al., 3D-Printable Bioactivated Nanocellulose–Alginate Hydrogels, ACS Appl. Mater. Interfaces. 9 (2017) 21959.

[35] M Müller, M Müller, E Öztürk, E Öztürk, Ø Arlov, Ø Arlov, et al. Alginate Sulfate–Nanocellulose Bioinks for Cartilage Bioprinting Applications, Ann Biomed Eng. 45 (2017) 210-223.

[36] T Möller, M Amoroso, D Hägg, C Brantsing, N Rotter, P Apelgren, et al. In Vivo Chondrogenesis in 3D Bioprinted Human Cell-laden Hydrogel Constructs, Plastic and reconstructive surgery. Global open. 5 (2017) e1227.

[37] ISO 1137-3-2018 Sterilization of health care products- Radiation-Part 1: Requirements for development, validation and routine control of a sterilization process for medical devices —Amendment 2: Revision to 4.3.4 and 11.2.

[38] Council of Europe. Chapter 2.6.1. Sterility. The European Pharmacopoeia, 9.0. ed.; EDQM: Strasbourg, France, 2017.

[39] A Zabala, L Blunt, R Tejero, I Llavori, A Aginagalde, W Tato. Quantification of dental implant surface wear and topographical modification generated during insertion, Surface Topography: Metrology and Properties. 8 (2020) 15002.

[40] ISO 25178-2 2012 Geometrical product specifications (GPS)—Surface texture: Areal: II.Terms, definitions and surface texture parameters, 2012.

[41] ISO 10993-5:2009 Biological Evaluation of Medical Devices. Part 5: Tests for In Vitro Cytotoxicity. International Organization for Standardization; Geneva, Switzerland: 2009.

[42] K Hölzl, S Lin, L Tytgat, S Van Vlierberghe, L Gu, A Ovsianikov. Bioink properties before, during and after 3D bioprinting, Biofabrication. 8 (2016) 032002.

[43] S Sakai, H Ohi, M Taya. Gelatin/Hyaluronic Acid Content in Hydrogels Obtained through Blue Light-Induced Gelation Affects Hydrogel Properties and Adipose Stem Cell Behaviors, Biomolecules. 9 (2019) 342.

[44] F Cilurzo, F Selmin, P Minghetti, L Montanari, C Lenardi, F Orsini, et al. Comparison between gamma and beta irradiation effects on hydroxypropylmethylcellulose and gelatin hard capsules, AAPS PharmSciTech. 6 (2005) E586-E593.

[45] WB Hugo. A brief history of heat, chemical and radiation preservation and disinfection, International Biodeterioration & Biodegradation. 36 (1995) 197-217.

[46] JA Bushell, M Claybourn, HE Williams, DM Murphy. An EPR and ENDOR study of γ- and β-radiation sterilization in poly (lactide-co-glycolide) polymers and microspheres, Journal of Controlled Release. 110 (2005) 49-57.

[47] L Montanari, F Cilurzo, F Selmin, B Conti, I Genta, G Poletti, et al. Poly(lactide-co-glycolide) microspheres containing bupivacaine: comparison between gamma and beta irradiation effects, Journal of Controlled Release. 90 (2003) 281-290.

[48] F EL-Ashhab, L Sheha, M Abdalkhalek, HA Khalaf. The influence of gamma irradiation on the intrinsic properties of cellulose acetate polymers, Journal of the Association of Arab Universities for Basic and Applied Sciences. 14 (2013) 46-50.

[49] E Daar, L King, A Nisbet, RB Thorpe, DA Bradley. Viscosity changes in hyaluronic acid: Irradiation and rheological studies, Applied Radiation and Isotopes. 68 (2010) 746-750.

[50] JG Prieto, MM Pulido, J Zapico, AJ Molina, M Gimeno, P Coronel, et al. Comparative study of hyaluronic derivatives: rheological behaviour, mechanical and chemical degradation, International Journal of Biological Macromolecules. 35 (2005) 63-69.

[51] A Maleki, A Kjøniksen, B Nyström. Anomalous Viscosity Behavior in Aqueous Solutions of Hyaluronic Acid, Polym. Bull. 59 (2007) 217-226.

[52] M Driscoll, A Stipanovic, W Winter, K Cheng, M Manning, J Spiese, et al. Electron beam irradiation of cellulose, Radiation physics and chemistry (Oxford, England : 1993). 78 (2009) 539-542.

[53] P Snetkov, K Zakharova, S Morozkina, R Olekhnovich, M Uspenskaya. Hyaluronic Acid: The Influence of Molecular Weight on Structural, Physical, Physico-Chemical, and Degradable Properties of Biopolymer, Polymers. 12 (2020) 1800.

[54] K.YongBok , K. GeunHyung. Collagen/alginate scaffolds comprising core (PCL)–shell (collagen/alginate) struts for hard tissue regeneration: fabrication, characterisation, and cellular activities, J. Mater. Chem. B. 1 (2013) 3185.

[55] F Yu, X Cao, Y Li, L Zeng, J Zhu, G Wang, et al. Diels–Alder crosslinked HA/PEG hydrogels with high elasticity and fatigue resistance for cell encapsulation and articular cartilage tissue repair, Polym. Chem. 5 (2014) 5116-5123.

[56] W Li, J Kang, Y Yuan, F Xiao, H Yao, S Liu, et al. Preparation and characterization of PVA-PEEK/PVA-β-TCP bilayered hydrogels for articular cartilage tissue repair, Composites Science and Technology. 128 (2016) 58-64.

[57] A Espona-Noguera, J Ciriza, A Cañibano-Hernández, L Fernandez, I Ochoa, L Saenz del Burgo, et al. Tunable injectable alginate-based hydrogel for cell therapy in Type 1 Diabetes Mellitus, International Journal of Biological Macromolecules. 107 (2018) 1261-1269.

[58] J Patterson, R Siew, SW Herring, ASP Lin, R Guldberg, PS Stayton. Hyaluronic acid hydrogels with controlled degradation properties for oriented bone regeneration, Biomaterials. 31 (2010) 6772-6781.

[59] S Tang, SM Vickers, H Hsu, M Spector. Fabrication and characterization of porous hyaluronic acid–collagen composite scaffolds, Journal of Biomedical Materials Research Part A. 82A (2007) 323-335.

[60] H Sung, C Meredith, C Johnson, ZS Galis. The effect of scaffold degradation rate on three-dimensional cell growth and angiogenesis, Biomaterials. 25 (2004) 5735-5742.

[61] M Farokhi, F Jonidi Shariatzadeh, A Solouk, H Mirzadeh. Alginate Based Scaffolds for Cartilage Tissue Engineering: A Review, International Journal of Polymeric Materials and Polymeric Biomaterials. 69 (2020) 230-247.

[62] Z Wu, X Su, Y Xu, B Kong, W Sun, S Mi. Bioprinting three-dimensional cell-laden tissue constructs with controllable degradation, Scientific reports. 6 (2016) 24474.

[63] H Park, B Choi, J Hu, M Lee. Injectable chitosan hyaluronic acid hydrogels for cartilage tissue engineering, Acta Biomaterialia. 9 (2013) 4779-4786.

[64] O Juffroy, D Noël, A Delanoye, O Viltart, I Wolowczuk, C Verwaerde. Subcutaneous graft of D1 mouse mesenchymal stem cells leads to the formation of a bone-like structure, Differentiation (London). 78 (2009) 223-231.

[65] J Kim, IS Kim, TH Cho, KB Lee, SJ Hwang, G Tae, et al. Bone regeneration using hyaluronic acid-based hydrogel with bone morphogenic protein-2 and human mesenchymal stem cells, Biomaterials. 28 (2006) 1830-1837.

[66] B Sayyar, M Dodd, L Marquez-Curtis, A Janowska-Wieczorek, G Hortelano. Fibronectin-Alginate microcapsules improve cell viability and protein secretion of encapsulated Factor IX-engineered human mesenchymal stromal cells, Artificial Cells, Nanomedicine, and Biotechnology. 43 (2015) 318-327.